Florence, Italy 12-16 July 2015
ICSV22
The 22nd International Congress on Sound and Vibration

EFFECT OF ORIFICE GEOMETRY ON THE NON-LINEAR ACOUSTIC RESISTANCE OF PERFORATED PLATES IN THE TRANSITION REGIME

Muttalip Aşkın Temiz[1]†, Jonathan Tournadre[2], Ines Lopez Arteaga[1], Paula Martínez-Lera and Avraham Hirschberg[3]

[1]*Eindhoven University of Technology, Dept. of Mechanical Engineering, Eindhoven, The Netherlands.*
† e-mail: m.a.temiz@tue.nl

[2]*Siemens Industry Software, Researchpark 1237, Interleuvenlaan 68, 3001 Leuven, Belgium*

[3]*Eindhoven University of Technology, Dept. of Applied Physics, Eindhoven, The Netherlands.*

With this study, we provide a global link between linear and non-linear acoustic resistance of a perforation as a function of orifice geometry and Strouhal number. High amplitudes of acoustic pressure induce flow separation at the edges of the orifices. This is a non-linear mechanism increasing the acoustic resistance of a perforation. Quasi-static models have been used to predict the acoustic resistance in the non-linear regime, yet the linear to non-linear transition has been out of focus so far. We carry out open-end impedance measurements in a semi-anechoic room with four different samples. These samples are selected to have different orifice geometries and edge profiles, so that the conclusions would be general. The most prominent result of this study is that the change in the non-linear resistance can be expressed as a function of the Strouhal number only, if the resistance is corrected for the *vena-contracta* factor which can be deduced from steady flow measurements.

1. Introduction

Perforated plates have various application areas in sound absorption, such as duct and architectural acoustics. Their sound absorption mechanism is often modeled by considering the resistance of a single perforation on the plate. When Sivian [1] reported that *strong* incident sound waves change this property, he introduced the *non-linearity* concept into acoustic response of perforations.

The pioneer work on non-linear acoustic response of a perforation has been carried out by Ingard and Ising [2]. They measured the pressure and the particle velocity amplitude upstream and inside an orifice, respectively. They reached $SPL = 157\,\mathrm{dB}$ ensuring that non-linear effects are dominant in their study. Yet, Ingard and Ising do not consider the *vena-contracta* factor of the orifice when they propose a quasi-static model for the non-linear resistance. Nevertheless, using a sharp-edged orifice in the measurements compensated this problem, leaving their result valid for circular perforations with sharp edge profile.

Later, Disselhorst and van Wijngaarden [3] carried out measurements of the radiation impedance of an open-pipe termination for rounded and square / sharp edge profiles. They found that vortex

shedding is the main mechanism for the non-linear acoustic response. They also provide an analytic model for vortex generation and shedding based on these experiments.

Cummings [4, 5], Hofmans *et al.* [6] and Jing and Sun [7] have improved the quasi-steady model for orifices of Ingard and Ising's [2] by introducing the *vena-contracta* factor. They also provide some theoretical and empirical values for the *vena-contracta* factor for circular orifices with square-edged and slit orifices with sharp-edged profiles.

Recently, Tonon *et al.* [8] have studied the perforations with chamfers. They investigated the quasi-steady acoustic response of the orifices. It should be noted that a more detailed study of the vortex shedding is provided by Leung *et al.* [9].

Although all of these studies provide very valuable information about the acoustic properties of a perforation in the non-linear regime, none of them focus on the linear to non-linear transition regime. This paper aims to provide a link between linear and non-linear acoustic resistance of a perforation by means of open-end transfer impedance measurements and the quasi-steady acoustic resistance model. To obtain general results, we use samples with four different orifice geometries and edge profiles.

2. Quasi-steady model for non-linear resistance

The acoustic non-linearity of an orifice (or perforation) subject to high amplitude harmonic oscillation is determined by the non-dimensional Strouhal number $Sr = 2\pi f d_p/|u_p'|$ where f is the frequency, d_p is the diameter of the perforation and $|u_p'|$ is the surface averaged acoustic velocity amplitude in the perforation [10]. For $Sr >> 1$ the acoustic response of an orifice is linear. If the acoustic particle displacement is comparable with the diameter of the perforation, *i.e.* $Sr \sim \mathcal{O}(1)$, the flow starts to separate and vortices form at the edges of the orifice. The perforation geometry and the parameters are sketched in Fig. 1.

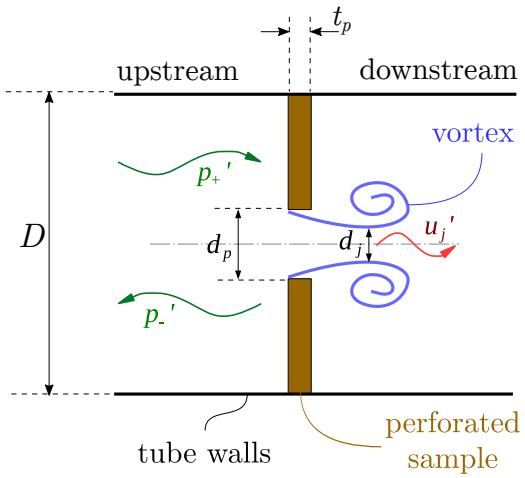

Figure 1: Typical orifice geometry. D is the diameter of the impedance tube, d_p is the perforation diameter, d_j is the diameter of the oscillating jet flow due to the *vena-contracta* effect, u_j' is the acoustic velocity in the jet area, t_p is the plate thickness.

Ingard and Ising [2] report for an orifice placed at the open end of a pipe that, when $|u_p'|$ exceeds some *transition* value, the upstream acoustic pressure amplitude $|p_u'|$ is proportional to the square of this velocity and the average density of the acoustic medium, ρ_0:

$$|p_u'| = \rho_0 |u_p'|^2. \tag{1}$$

According to Ingard and Ising's experiments, this transition velocity amplitude is around 10 m/s. Considering their set-up and sample specifications ($d_p = 7$ mm, $f = 150$ Hz) this transition velocity

amplitude corresponds to $Sr = 0.66$. For the perforation velocity amplitudes larger than this transition value, the acoustic resistance becomes almost equal to the transfer impedance amplitude of the perforation, $\Re\{Z_t\} \approx |Z_t|$. In this region, the quasi-steady approach is valid.

Although Ingard and Ising [2] did not consider the jet forming in low Sr number region, this does not invalidate their findings for their specific test case, but limits their result to sharp-edged orifices. Considering the flow sketched in Fig. 1, the pressure difference $\Delta p'$ across the perforation [6] is:

$$\Delta p' = \frac{1}{2}\rho_0 (u_j')^2. \tag{2}$$

The amplitude of the jet velocity is related to the acoustic velocity amplitude in the perforation, $|u_p{}'|$, as follows:

$$u_j{}' = \frac{|u_p{}'|}{C_{vc}}, \tag{3}$$

where C_{vc} is the *vena-contracta* factor. One finds $C_{vc} = 0.61$ for the orifices with sharp or square-edged profiles and $0.95 < C_{vc} < 1.0$ for rounded or chamfered edges [7, 8].

Combining Eqs. (2) and (3), we can generalize Eq. (1) for different edge profiles.

$$|\Delta p'| = \frac{1}{2C_{vc}^2}\rho_0 |u_p'|^2. \tag{4}$$

Our study in the linear to non-linear transition regime is based on this approach and proposes a correction factor connecting these regimes.

3. Experimental set-up

The experimental investigation of the mentioned quasi-steady model is performed on an impedance tube workbench. The impedance tube and the measurement method are sketched in Figure 2.

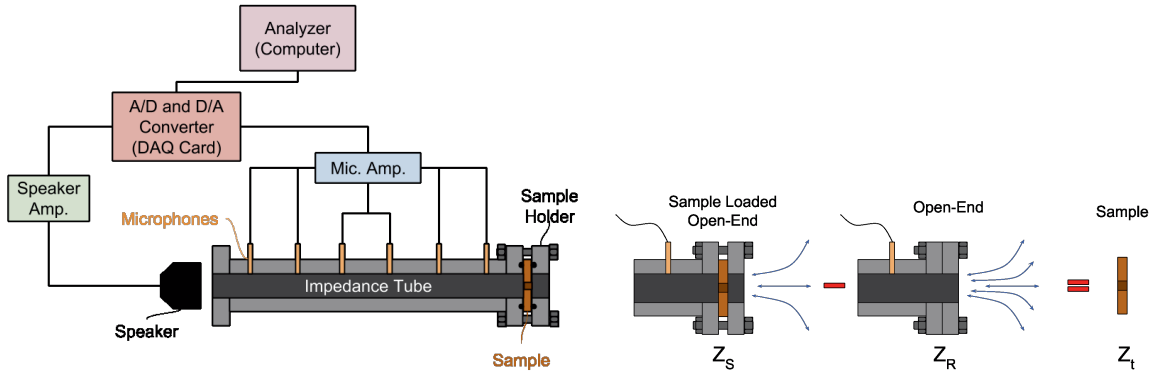

(a) Impedance tube.

(b) Open-end transfer impedance measurement method.

Figure 2: Description of the experimental set-up (a) and the measurement procedure (b). The difference between sample loaded termination impedance, Z_S, and open termination impedance, Z_R, gives the transfer impedance of the plate, $Z_t = Z_S - Z_R$.

The tube shown in Fig. 2a is 1-m long and the inner diameter is $D = 50\,\text{mm}$. Along the tube, there are 6 *BSWA MPA416* microphones that are placed equidistantly. The distance between two neighbouring microphones is $175\,\text{mm}$ and their sensitivity is about $50\,\text{mV/Pa}$.

We perform signal processing and data acquisition with the combination of an *NI PCIe-6361 X-Series* DAQ card and LabView®. The sampling frequency for the generated excitation signal is 20 kHz where the recording sampling frequency is 10 kHz. For each frequency step, we record the data for 10 seconds and trim the first and last 2 seconds to exclude transient effects. The recorded pressure data is transformed into the Frequency domain with a Lock-in method. A separate Matlab® script has been built for this post-processing.

We calibrate the microphone that is closest to the sample with a B&K pistonphone at 1000 Hz. The rest of the microphones are calibrated relatively to this reference microphone. To do that, we place all the microphones near to a closed end wall at the same distance with respect to the speaker and for each frequency step in the region $100\,\text{Hz} < f < 700\,\text{Hz}$, a calibration coefficient is measured relative to a reference microphone.

For non-linearity considerations, the amplitude of the acoustic pressure in the tube is measured at the reference microphone and wave decomposition is performed as explained in [11].

To avoid a temperature gradient inside the tube, after each 20 frequency-steps, we wait 15 minutes for the temperature to be uniform again.

With all of the precautions and methods employed, in the frequency range of $100\,\text{Hz} < f < 700\,\text{Hz}$, the deviation from the theoretical value is less than 0.5% for closed-end reflection coefficient measurements. Yet, we perform open-end measurements to calculate the transfer impedance of an MPP sample. The idea behind the *open-end transfer impedance measurement* is illustrated in Figure 2b.

We perform open-end measurements in a semi-anechoic room to minimize the effect of ambiance. Since both the *open-end* and *sample loaded open-end* measurements are carried out in the same medium, we expect the resistance part of the radiation impedance to be the same for both of the cases. Moreover, as the porosity of the samples are in the order of 1%, the transfer impedance of the samples are expected to be much larger than the radiation impedance.

The geometry and the specifications of the samples used in the experiments are given in Fig. 3.

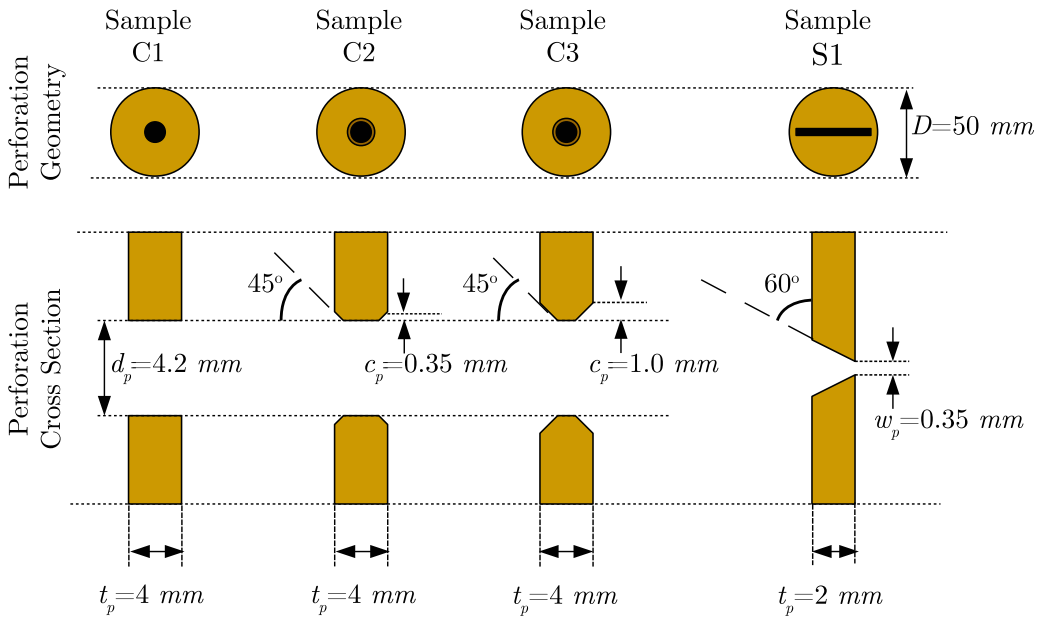

Figure 3: Sketch of the samples with their geometric specifications. Samples C1, C2 and C3 have circular geometries where Sample S1 has a slit geometry. The porosity is the same for all circular samples, *i.e.* $\sigma_{C1} = \sigma_{C2} = \sigma_{C3} = 0.007$; where for the slit sample it is $\sigma_{S1} = 0.008$.

Samples C1, C2 and C3 differ from each other by their edge profiles. C1 has the square-edged geometry, where C2 and C3 has a chamfer-edged profile. The difference between C2 and C3 is their chamfer size as shown in Fig. 3. Lastly, Sample S1 has the slit shaped orifice with a taper from one

end to another. The length of the slit is $L_p = 48\,\text{mm}$. To be able to compare Sample S1 with the other samples, we define the hydrodynamic diameter of the slit area as $d_h = 2\sqrt{(w_p L_p)/\pi}$. One should consider replacing d_p with d_h when calculating the non-dimensional parameters, such as Sr, for Sample S1 in this study.

4. Results and discussions

The flow separation initiates when Sr is of the order of unity. This is called the *transition regime*. If the perforation thickness is long enough, the flow reattaches to the wall [12]. To avoid this phenomenon, thin plates, *i.e.* $d_p/t_p > 0.5$, are used in the experiments as can be seen in Fig. 3.

Even though the non-linear effects dominate the resistance of a perforation in the region $Sr << 1$, linear and non-linear contributions to the resistance are comparable in the transition region. To focus only on the non-linear effects, we subtract the linear contribution of the resistance, $\Re\{Z_t\}_L$ from the resistance measured in the transition regime, $\Re\{Z_t\}_{NL}$. $\Re\{Z_t\}_L$ is the measured value obtained at $Sr \sim \mathcal{O}(10^2)$. Moreover, to be able to compare this quantity with the non-linear resistance, we divide this difference by Ingard and Ising's quasi-steady model [2] given by Eq. (1). Finally, since we measure the impedance in the tube, we multiply this term with the porosity, σ, to obtain the dimensionless non-linear resistance of the perforation as follows:

$$\Delta R_{NL} = \frac{(\Re\{Z_t\}_{NL} - \Re\{Z_t\}_L)\sigma}{\rho_0 |u_p'|}. \tag{5}$$

After defining the non-linear resistance difference in Eq. (5), we investigate the effect of the Shear number, Sh, which is a dimensionless parameter for comparing the Stokes boundary layer thickness and the perforation diameter. It is defined by Peters *et al.* [10] as $Sh = d_p\sqrt{(\omega\rho_0)/(4\mu)}$, where $\omega = 2\pi f$ is the radial frequency and μ is the dynamic viscosity of air. The effect of Sh is examined only for Sample C1. ΔR_{NL} values are plotted as a function of $1/Sr$ in Fig. 4 for various Sh values corresponding to 120, 140, 160, 180 and 220 Hz.

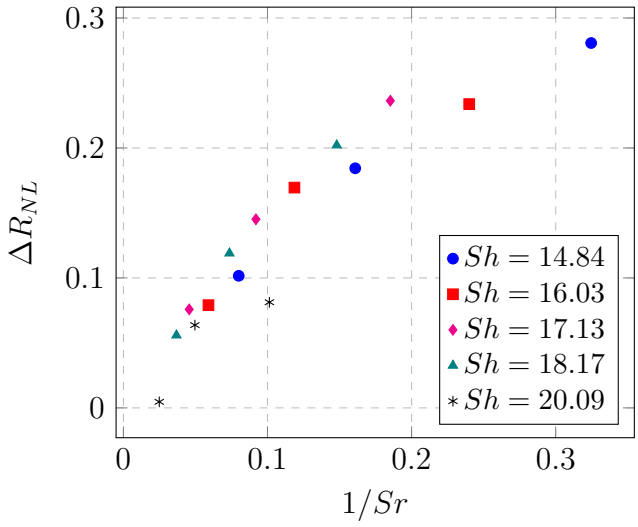

Figure 4: The Shear number effect on non-linear resistance difference for $Sh > 10$. Sh does not have a strong effect on ΔR_{NL}.

Two main observations can be drawn from Fig. 4. Firstly, for a certain geometry ΔR_{NL} is not strongly affected by the change in Sh. Considering that the Stokes boundary layers are responsible of the *linear* resistance in the perforations [13], this result confirms that the parameter we define in Eq. (5) represents only the non-linear behaviour. Secondly, we see that $\Delta R_{NL} \sim \mathcal{O}(0.1)$. This is due

to the fact that our measurements are in the transition regime. In the non-linear regime, $\Re\{Z_t\}_{NL} - \Re\{Z_t\}_L \approx \Re\{Z_t\}_{NL}$ would hold and, $\Delta R_{NL} \sim \mathcal{O}(1)$.

Furthermore, we study the perforation geometry and edge profile effects on the non-linear resistance change. In Fig. 5a we compare all the samples for different Sr numbers at 120 Hz.

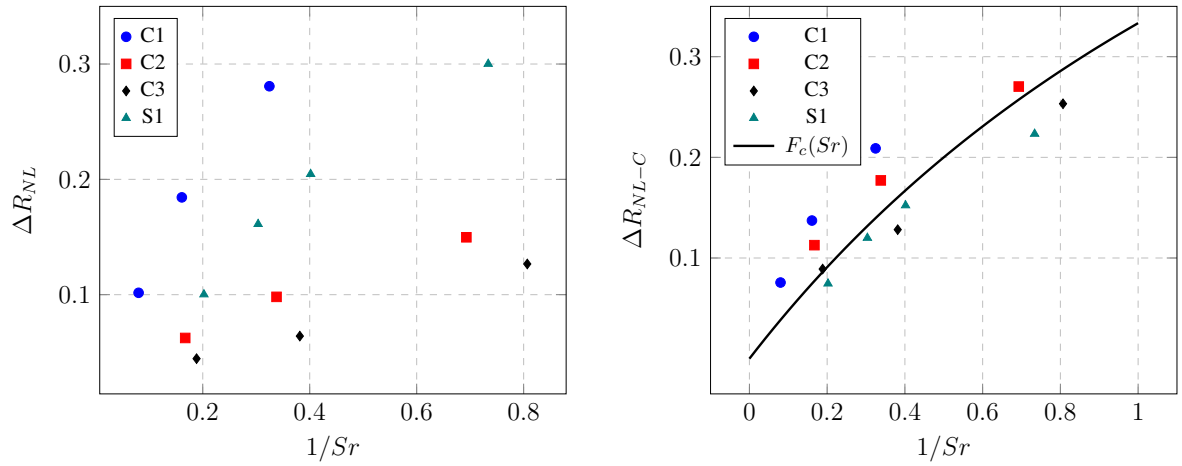

(a) Effect of perforation geometry and edge profile. The samples with the chamfer-edged profile (C2 and C3) experience less non-linear effects than square-edged profile (C1). On the other hand, the non-linear resistance difference of the sample with slit geometry, S1, is comparable to C1.

(b) Non-linear resistance difference for different geometries corrected for the *vena-contracta*. Regardless of the geometry, all samples display a very similar non-linear behaviour. This behaviour is modeled as $F_c(Sr) = 1/(2Sr + 1)$ and plotted as a solid line.

Figure 5: Comparison of the non-linear resistance difference of various geometries at 120 Hz.

From Fig 5a, it is seen that the edge profile and the perforation geometry are important for the non-linear resistance difference. But these effects can be compensated by adopting Cummings' quasi-steady approach for the effect of the *vena-contracta* factor [4]. The key point in this procedure is to define the *vena-contracta* factor, C_{vc}, correctly. Emprical data is provided by Cummings[4] and Jing and Sun [7]. In principle, C_{vc} can also be measured from steady flow experiments [14]. By Eq. (4), the corrected non-dimensional resistance difference ΔR_{NL-C} is calculated by

$$\Delta R_{NL-C} = \Delta R_{NL}\, 2\, C_{vc}^2, \tag{6}$$

and plotted in Fig. 5b. The C_{vc} values chosen for these samples are given in Table 1.

Table 1: Corresponding *vena-contracta* factors for the samples used in the measurements.

Sample	C1	C2	C3	S1
C_{vc}	0.61[1]	0.95	1.00	0.61

Once the geometry effect is compensated for the *vena-contracta* factor, we observe that ΔR_{NL-C} depends mainly on Sr in Fig. 5b. In other words, this quantity can be related to the linear ($Sr >> 1$) and non-linear ($Sr << 1$) regimes by means of a correction function, $F_c(Sr)$. The upper and lower limits for $F_c(Sr)$ must satisfy

$$\lim_{Sr\to\infty} F_c(Sr) = 0, \tag{7a}$$

$$\lim_{Sr\to 0} F_c(Sr) = 1, \tag{7b}$$

[1]Cummings [4] suggests $C_{vc} = 0.75$ for square-edged circular perforations. On the other hand, Jing and Sun [7] report that $C_{vc} = 0.61$ fits their measurements better.

so that the non-linear resistance diminishes in linear regime and becomes dominant in the non-linear regime.

The function $F_c(Sr) = 1/(2Sr + 1)$ satisfies the conditions given in Eq. (7) and represent the distribution of the measured points in Fig. 5b fairly well. Using this function, the non-linear resistance difference is calculated as a function of geometry and Sr as

$$\Delta R_{NL} = \frac{1}{(2\,C_{vc}^2)(2Sr + 1)}. \tag{8}$$

5. Conclusions

This study focused on the linear to non-linear transition regime in perforations, *i.e.* $1 \leq Sr \leq 10$. In this regime, we investigate the effects of the Strouhal number, Sr, and the orifice geometry on the acoustic non-linearity of the perforations. We have carried out *open-end transfer impedance measurements* to obtain the acoustic resistance of the perforations.

In the region of $Sh \geq 10$, our measurements show that the dimensionless non-linear resistance difference of the perforation does not depend strongly on the Sh number. Yet, the question "Does the Sh number have an effect on the resistance in the typical Sh range for micro-perforated plates, *i.e.* $1 < Sh < 10$?" needs further investigations.

Furthermore, we observe that the perforation geometry and the edge profile is important in terms of non-linear resistance. The difference caused by the geometry can be predicted using the quasi-steady theory in combination with the *vena-contracta* factor. This way, *geometrically corrected* non-linear resistance difference becomes a function of Sr only.

Our main result is a simple but global correlation for the transition regime that relates linear resistance to non-linear resistance as a function of orifice geometry and Sr.

Acknowledgments

The presented work is part of the Marie Curie Initial Training Network Thermo-acoustic and aero-acoustic non-linearities in green combustors with orifice structures (TANGO). We gratefully acknowledge the financial support from the European Commission under call FP7-PEOPLE-ITN-2012.

REFERENCES

1. Sivian, L. J. Acoustic Impedance of Small Orifices, *Journal of Acoustical Society of America*, **7**, 94–101, (1935).

2. Ingard, U. and Ising, H. Acoustic Nonlinearity of an Orifice, *Journal of Acoustical Society of America*, **42**(1), 6–17, (1967).

3. Disselhorst, J. H. M., van Wijngaarden L. Flow in the exit of open pipes during acoustic resonance, *Journal of Fluids and Structures*, **90**(2), 293–319, (1980).

4. Cummings, A. Acoustic nonlinearities and power losses at orifices, *AIAA Journal*, **22**(6), 786–792, (1984).

5. Cummings, A. Transient and multiple frequency sound transmission through perforated plates at high amplitude, *The Journal of the Acoustical Society of America*, **79**(4), 942–951, (1986).

6. Hofmans, G. C. J., Boot, R. J. J., Durrieu, P. P. J. M., Aurégan, Y. and Hirschberg, A. Aeroacoustic Response of a Slit-Shaped Diaphragm in a Pipe at Low Helmholtz Number, 1: Quasi-Steady Results, *Journal of Sound and Vibration*, **244**(1), 35–56, (2001).

7. Jing, X., Sun X., Sound-excited flow and acoustic nonlinearity at an orifice, *Physics of Fluids*, **14**(1), 268–276, (2002).

8. Tonon, D., Moers, E. M. T. and Hirschberg, A. Quasi-Steady Acoustic Response of Wall Perforations Subject to a Grazing-Bias Flow Combination, *Journal of Sound and Vibration*, **332**, 1654–1673, (2013).

9. Leung, R C. K., So R. M. C., Wang M. H., and Li, X. M. In-duct orifice and its effect on sound absorption, *Journal of Sound and Vibration*, **299**, 990–1004, (2007).

10. Peters, M. C. A. M., Hirschberg, A., Reijnen, A. J. and Wijnands, A.P.J. Damping and reflection coefficient measurements for an open pipe at low Mach and low Helmholtz numbers, *Journal of Fluid Mechanics*, **256**, 499–534, (1993).

11. Temiz, M. A., Lopez Arteaga, I., Hirschberg, A. Sound Absorption Measurements for Micro-Perforated Plates: The Effect of Edge Profile, *Proceedings of EURONOISE 2015*, Maastricht, The Netherlands, 31 May–3 June, (2015).

12. Testud, P., Moussou, P., Hirschberg, A., Aurégan, Y. Noise generated by cavitating single-hole and multi-hole orifices in a water pipe, *Journal of Fluids and Structures*, **23**(2), 163–189, (2007).

13. Temiz, M. A., Lopez Arteaga, I., Efraimsson, G., Mats, A., Hirschberg, A. Acoustic End-Correction in Micro-Perforated Plates - Revisited, *Proceedings of ICSV 21*, Beijing, China, 13–17 July, (2014).

14. Blevins, R. D. *Applied Fluid Dynamics Handbook*, Van Nostrand Reinhold, NY, (1984).